Int. J. Simul. Multidisci. Des. Optim. **14**, 20 (2023)

https://doi.org/10.1051/smdo/2023012

IJSMDO
Available online at:
https://www.ijsmdo.org

RESEARCH ARTICLE OPEN ACCESS

Parameters optimization in plasma arc cutting of AISI 1020 mild steel plate using hybrid genetic algorithm and artificial neural network

Nebyu Silabat Melaku and Teshome Mulatie Bogale*

Mechanical Engineering Department, Bahir Dar Institute of Technology, Bahir Dar University, Bahir Dar, Amhara, Ethiopia

Received: 19 June 2023 / Accepted: 31 August 2023

Abstract. The aim of this study was to optimize the cutting parameters such as cutting speed, standoff distance, cutting current and gas pressure of the CNC plasma arc cutting process that affected the material removal rate, surface roughness and nozzle diameter change after cutting performed on AISI 1020 mild steel plate. Three levels of variation were taken to the four cutting parameters that were chosen. Twenty-seven trial experiments were carried out using L27 orthogonal array of Taguchi design. In this experimental investigation, the highest material removal rate (MRR) of 8.96 g/s, Ra surface roughness (SR) of 15.734 μm and nozzle orifice diameter (ND) of 1.4637 mm were achieved, whereas the lowest obtained values of MRR, SR and ND were 2.324 g/s, 5.98 μm and 1.2114 mm, respectively. For modeling the plasma arc cutting process experimental input parameters and responses' results, a hybrid ANN-GA model was constructed. This model was used to forecast and optimize MRR, SR and ND, as well as the control factors that go with it. The results indicated that the ANN-GA model could predict the output responses with a mean square error of 1.06885e–1. During optimization, a 4-9-3 network trained with neural network of back propagation by Levenberg-Marquardt algorithm was used to have the greatest prediction capability, with optimum values of MRR, SR and ND of 7.0032 g/s, 4.2062 μm and 1.3142 mm, respectively. From the confirmation tests, the average results of 6.9247 g/s of MRR, 4.3429 μm of SR and 1.3703 mm of ND were obtained. The percentage of errors between the ANN-GA predicted optimal responses' results and the confirmatory experimental results were found 1.121%, 3.250% and 4.269% for MRR, SR and ND, respectively.

Keywords: Material removal rate / nozzle diameter / surface roughness / artificial neural network / genetic algorithm / plasma arc cutting parameters

1 Introduction

Plasma arc cutting is the process that melts and cuts metal by using a confined jet of high temperature plasma gas [1,2]. R. Gate patented this approach in 1957. The process was first used to cut difficult to machine materials, but it was later expanded to include a wide range of other manufacturing processes that demand high thermal energy concentrations, like coating, welding, heat treatment, and so on. The potential of plasma arc cutting to compete with laser cutting has boosted the attention of modern industries in applications of plasma arc cutting [3,4]. In contrast to flame cutting, which is the combustion process, plasma cutting is the melting technique. The material in the kerf is melted and expulsed by a gas jet in the plasma. An electric arc forms between an electrode and a workpiece during the operation. The arc formed between the work piece and the electrode, which becomes ionized and escapes via a nozzle's pin hole. The high-temperature arc, which reaches temperatures of over 18,000 °C, is ionized and penetrates deeply into a conductive substance through a narrow nozzle with high-pressurized air [5]. In a torch, the electrode tip is inserted into water or air-cooled gas nozzle. The nozzle is used to conduct the plasma gas. The arc and the plasma gas must flow through a very small aperture in the nozzle's tip. The gas is ionized and heated. Heat is transmitted to the work piece when the plasma jet collides with it owing to recombination. A passage of gas melts the material and expels it from the kerf. A pilot arc must be created to start the process and ionize the gas. The pilot arc warms and ionizes the plasma gas. The main arc ignites and the pilot arc extinguishes automatically because the main arc's electrical resistance is lower than the pilot arc's [6].

* e-mail: teshomemul@gmail.com

The cutting parameters of plasma arc cutting process have impacts on the cutting quality, nozzle wear rate and production rate on which their levels have been set. The effects of these parameters are explained as the followings. The nozzle is placed at a distance that to prevent the nozzle from contacting with the metal, which might result in the tip being destroyed quickly during the cutting operation. As a result, it appears that selecting appropriate machining conditions, such as torch height, gas pressure, and cutting speed is crucial for maximizing the efficiencies of such machining operations [7]. Cutting current is the current amount supplied to the process of plasma arc cutting when cutting a work piece; it affects cutting power. In the research [8] that was carried out to identify the best ideal combination of three process parameters of a CNC plasma arc cutting machine during cutting mild steel with a thickness of 12 mm for the response values of kerf width and material removal rate, the current values of 65, 85 and 105 A were considered. As the design of the experiment, the experiment was performed using Taguchi's L9 orthogonal array. Results were analyzed using S/N ratio, and analysis of mean (ANOM) was used for deciding which parameter had more effect on the responses. The results showed that an optimal cutting current of 85 A produced a response value of 2.246 mm kerf width and 151.119 g/min material removal rate. Another study [9] provided an experimental examination of the top kerf width, material removal rate, bottom kerf width, and bevel angle response of the plasma arc cutting process on structural steel using four process parameters. The values of cutting current were 30, 35 and 40 A. The experiment was designed using Box-Behnken response surface methodology (RSM), and process parameters were optimized using grey relational analysis, and an optimal cutting current of 40 A with a material removal rate of 3188.66 mm^3/min was obtained. Cutting speed refers to the plasma cutting torch's speed. An experiment was carried out by evaluating four plasma arc cutting parameters on EN-45A with a thickness of 12 mm in order to investigate their influences on the material removal rate [10]. The taken cutting speeds in this article were 280, 300, 320 and 340 mm/min. The Taguchi technique was employed to design the experiment the L16 orthogonal array. ANOVA was also employed in the study to determine the percentage contribution of each parameter. Finally, the material removal rate of 0.9452 cm^2/s was obtained at an ideal cutting speed of 340 mm/min, and cutting speed had the greater influence on material removal. The study [11] was conducted to investigate the influence of four process parameters on CNC plasma arc cutting utilizing 10 mm thick mild steel with the responses of material removed, surface roughness, and nozzle wear as outputs. In this article, cutting speeds of 400, 500, 600 and 700 mm/min were considered. The experiment yielded the best results of material removed of 0.629 g, surface roughness of 0.008 m, and nozzle wear of 62.48 mm at a cutting speed of 700 mm/min. AISI 1018 mild steel was used as the working material for the study [6] and four plasma arc cutting parameters were chosen to investigate their influence on responses, such as surface roughness, material removal rate, and heat-affected zone (HAZ). The cutting parameter of gas pressure was set to 4, 6, 8, and 10 bars. The experiment was planned using Taguchi's L16 orthogonal array, and grey relational analysis was used to optimize the cutting settings. ANOVA was also utilized to predict the impact of each process parameter on each output response. From this optimization and experimental works, the ideal material removal rate of 4.90 g/s and surface roughness of 2.98 m were attained at the gas pressure of 10 bar. The effect of three cutting parameters of CNC plasma arc cutting of 5 mm thick mild steel with an output response of kerf width and surface roughness was also investigated [12]. The considered gas pressures were 5, 5.5, and 6 bars. The experiment was designed via the Box-Behnken approach of RSM. For obtaining an optimal parameter S/N ratio graph, main effect graph and contour plots were used. In the study, ANOVA was also used for knowing the percentage contribution of the parameters. The optimum gas pressure of 5 bar was obtained for getting surface roughness of 2.3 μm. The effect of CNC plasma arc cutting parameters on material removal rate (MRR) by utilizing 10 mm thickness of mild steel was studied [13]. Standoff distance of 5, 6 and 7 mm were taken as cutting parameters' levels-settings. The Taguchi's L9 orthogonal array was used for designing the experiment, and the cutting parameter optimization was done by computing the S/N ratio of Taguchi method. The optimal material removal rate was 77.40 g/s at standoff distance 7 mm. Cutting factors including current, gas pressure, and cutting speed all had effects on nozzle wear [14]. Generally, the effects of cutting parameters of plasma arc cutting process were investigated as explained before.

From the previous researches, it was observed that most of parameters of plasma arc cutting process were optimized and identified their effects using Taguchi method, RSM, grey relational analysis, S/N ratios, ANOVA and ANOM. And, the experimental works were carried out based on orthogonal arrays of Taguchi design and design of RSM. However, the previously used optimization methods were not effective since they could only give discrete optimal results, Taguchi method is only used to optimize single response, and all the above-mentioned methods have lower prediction capacities than the hybrid artificial neural network and genetic algorithm. A design of experiment (DOE) in an experimental investigation reduces the number of experiments and the time it takes to complete the research [15–17]. An orthogonal array is utilized in the Taguchi design to reduce the number of experimental runs required to determine the optimal parameters of machining process [16]. Artificial neural network (ANN), is a network of nodes that is inspired by biological neural networks. In terms of a computing system, the analyses performed by ANNs are comparable to those performed by animal or human brains [18]. Using a simplified model, an ANN may transfer signals between many nodes known as artificial neurons. The connections that occur between neurons are referred to as edges. A neuron takes a real-number signal, analyzes it, and evaluates the output using a non-linear function of the summation of its inputs. Weights on edges and neurons change as learning continues, and these weights can either increase or decrease signal intensity at a connection. Layers of neurons are linked together, and each layer can perform

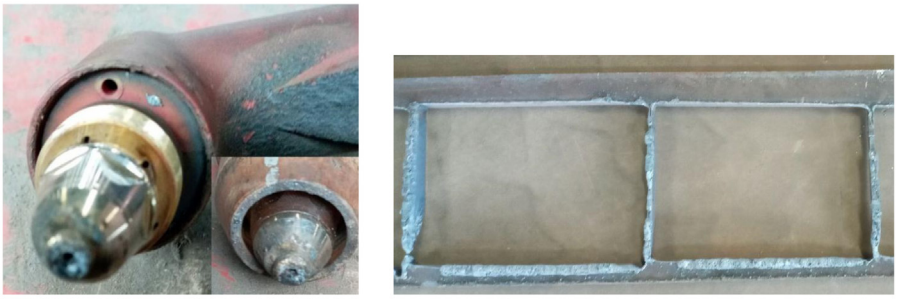

(a) nozzle wear (b) low quality cut

Fig. 1. Observed defects in the AMIMTDE company.

various changes on the information it receives [19]. Besides, genetic algorithm (GA) is used to discover the optimal solution to a given computing issue that minimizes or maximizes a certain function [1]. GA are one aspect of the field of research called as evolutionary computation because they mimic the natural selection and reproduction of biological processes to solve for the 'fittest' answers. In a genetic algorithm, many processes are random, much as in evolution, however this optimization approach allows you to govern and control the amount of unpredictability. These algorithms are far more efficient and powerful than random and exhaustive search methods, and they do not require any extra issue information. This property enables them to tackle problems that conventional optimization methods cannot because of a lack of derivatives, continuity, linearity, or other qualities [20]. As a consequence, the GA searches through the number of solutions in the search space, constantly searching for the global optimum, the individual with the best prospects [21].

In cutting of AISI 1020 mild steel mild steel plate with plasma arc cutting machine was difficult in the Amhara Metal Industry and Machine Technology Development Enterprise (AMIMTDE), due to the continuous failure of the nozzle. The nozzle of the plasma arc cutting machine was worn quickly without cutting the required amount of cut length as shown on Figure 1a. Most cutting operations were performed with having great trouble because the quality of the cut and the accuracy were very low as shown on Figure 1b. The combined effects of a continuous failure of the nozzle and low quality of cutting were leading large amount of failure on the quality of product during working time. The main reason for failure was the incorrect combination of cutting parameters' setting of levels.

There were not related researches that were conducted to address the observed problems in the AMIMTDE company; As a result, the basic objective of this study was to optimize the cutting parameters of plasma arc cutting process to improve surface roughness and material removal rate and reduce nozzle orifice diameter change after cutting performed on AISI 1020 mild steel plate on plasma arc cutting machine using hybrid genetic algorithm (GA) and artificial neural network (ANN). The simple flow chart is shown on Figure 2 to represent the steps-wise procedure that was followed for carrying out both the design optimization and experimental method.

2 Materials and methods

2.1 Materials

The material composition test was investigated using metal analytic spectrometer machine having model of MAXx LMD06, and the result of the composition test was presented on Table 1. From these test results, it was observed that carbon content was 0.207, so this value is in a ranges for mild steel. Since mild steel has a carbon content range from of 0.05 to 0.25%. Mild steel is the least expensive of all steels since it is the most widely used. Mild steel is used in almost every steel product that is manufactured. Mild steel is tough and long-lasting, but it's prone to rust, so it needs to be painted or coated to keep it from corroding.

The experiment was carried out on $60 \times 30 \times 10$ mm AISI 1020 mild steel by cutting it from $400 \times 90 \times 10$ mm plate as shown its CAD model on Figure 3a. The plasma cutting machine that was used for cutting the specimens in this experimental study was the EDON CUT-100 machine. The path for cutting of the specimens was given by specifying the required dimension, which is $60 \times 30 \times 10$ mm as shown in Figure 4a. By setting levels like giving the value of current on the power supply, changing the gas pressure on the air compressor, setting the cutting speed on the CNC controller unit and adjusting the standoff distance on the controller, cutting off three $60 \times 30 \times 10$ mm specimens were performed on each $400 \times 90 \times 10$ mm and this process is shown on Figure 4b. The final prepared specimens are shown on Figure 3b.

2.2 Methods

2.2.1 Cutting parameters and orthogonal array selections

Selection of the control cutting parameters of plasma arc cutting process were done by taking the actual cutting parameters in the AMIMTDE company while cutting 10 mm thickness of AISI 1020 mild steel plate and by referring different researches that were done on mild steel using plasma arc cutting process. The actual working parameter values for cutting 10 mm thickness of AISI 1020 mild steel plate, which the company usually used, were evaluated. This aided in determining the machine ranges for power supply, compressor, and speed modification, as well as producing a result within an acceptable range, because those literature reviews were focused on mild steel

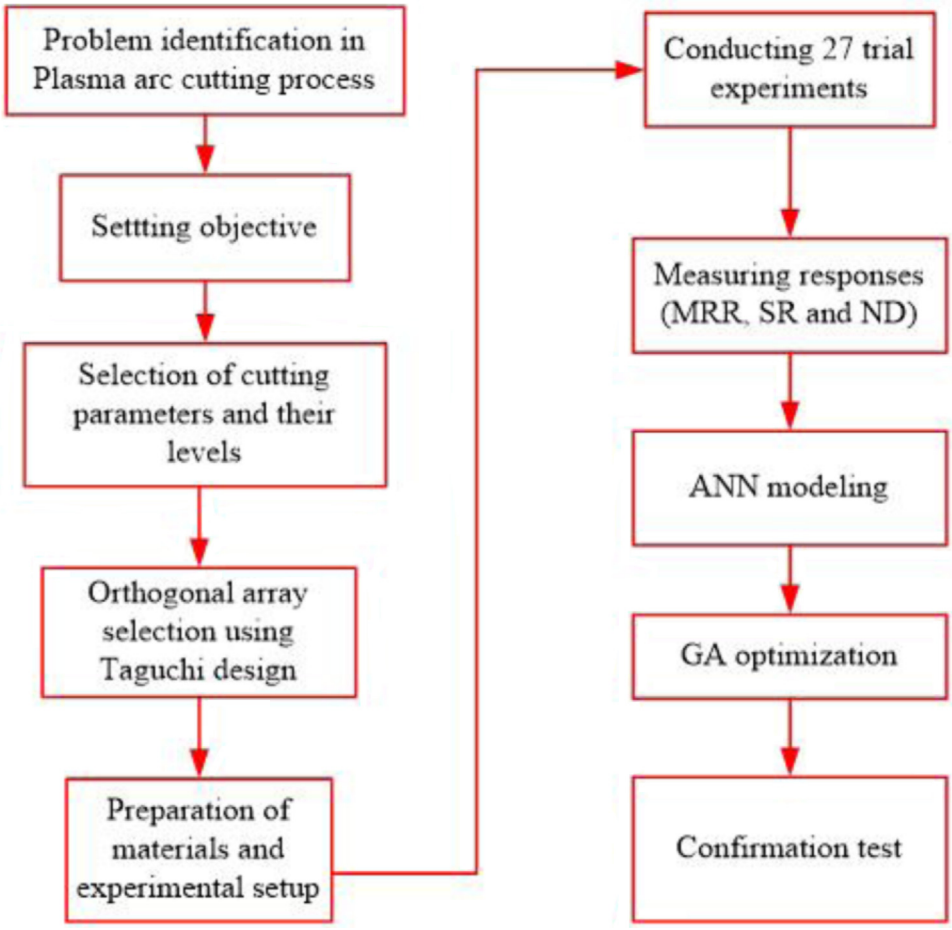

Fig. 2. Flowchart of the design optimization and experimental method.

Table 1. AISI 1020 mild steel plate chemical composition.

Material	Fe	C	Si	Mn	Cu	S	P	Sn	Others
Composition (%)	98.2	0.207	0.176	0.393	0.409	0.077	0.070	0.157	0.311

cutting and contained responses that were taken into account in this study. Accordingly, the most important control cutting parameters were chosen using Pareto chart as shown on Figure 5. The first four parameters were chosen as cutting parameters since they cumulatively contribute 80.6% which is more than 80%, each having its unique effect on the cutting quality, while the remaining parameters were kept as constants. As results, the control parameters were current, speed, gas pressure, and standoff distance for cutting the selected metal to forecast material removal rate, surface roughness and nozzle diameter change. The levels of selected cutting parameters shown on Table 2 were also chosen based on the specifications of plasma cutting machine which was utilized in this study and by reviewing previous researches that were in the same context as the cutting parameter decision [22–24].

Actually, many Taguchi designs are founded on factorial designs of 2-level designs, Plackett and Burman designs, and factorial designs with more than 2 levels. However, Taguchi's designs are typically highly fractionated, making them appealing to practitioners. A half, quarter or eighth fraction of a full factorial design minimizes the cost and time required for a proposed experiment significantly. In this study, four factors with their three levels were taken. According to Taguchi design, the available recommended designs are L9 and L27 orthogonal arrays. The L9 has the advantages of both maximum and minimum trial runs, was provided to minimize the number of runs [25]. By taking consideration of better prediction during ANN model, L27 was selected even though L9 was enough in terms of cost [16]. However, the possible runs would be 81 in factorial design with single

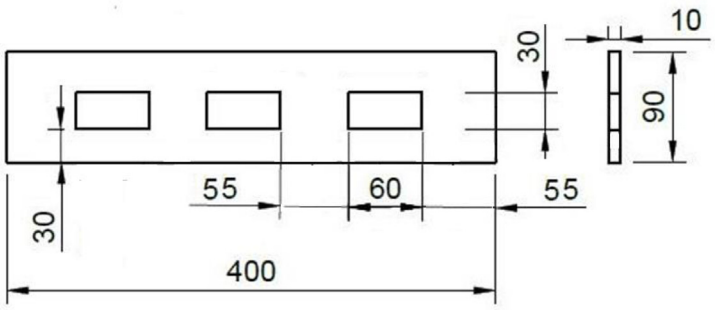

(a) CAD model of the specimens (mm)

(b) after cutting specimens

Fig. 3. Preparation of specimens.

(a) cutting path specification

(b) cutting of 60×30×10 mm specimen

Fig. 4. Experimental setup on EDON CUT 100.

replication. Orthogonal array is another expression of Taguchi design for the experimental layout of levels of design parameters. So, the L27 orthogonal array had been selected, and it is shown on Table 3.

2.2.2 Measurement of responses

For knowing the material removal rate, the mass of the workpiece was measured. After completing the cutting of nine $400 \times 90 \times 10$ mm AISI 1020 mild steel plate on EDON CUT 100 plasma arc cutting machine, measurement of initial mass before cutting of each specimen one by one was recorded using JSC-D7 model WEIGHING INDICATOR device as shown on Figure 6. The value of material removal rate was obtained from the mass difference between before and after cutting of specimen and divided by the time it took while cutting the specimens. The measured results of mass before and after cutting the plate and the time it took are shown on Table 3.

Surface roughness (Ra) is the arithmetical mean of all profile values added together. Ra is by far the most often utilized metric for surface finish measurement and quality management in general. Despite its limitations, it is simple to measure and provides a decent overall representation of

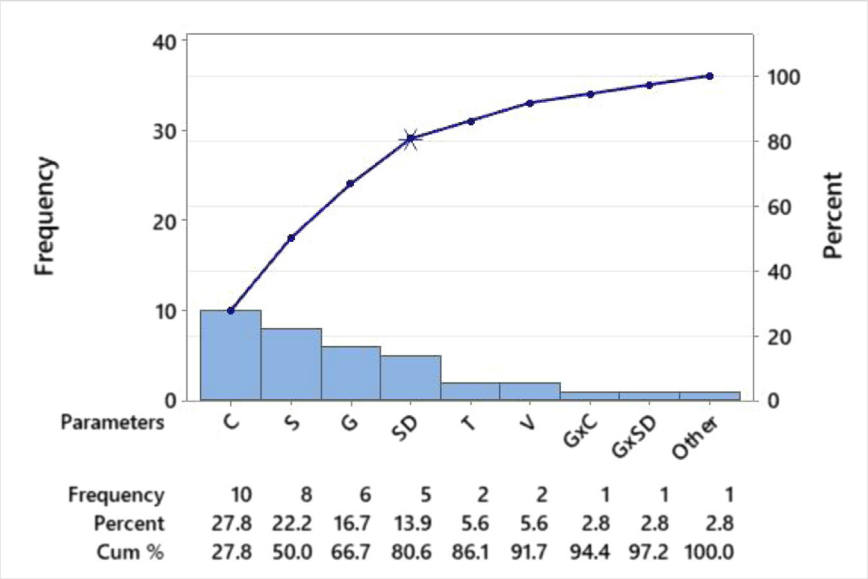

Fig. 5. Pareto chart of parameters (C = current, S = speed, G = gas pressure, SD = standoff distance, T = thickness, and V = voltage).

Table 2. Cutting parameters and their levels.

Parameters	Levels		
	1	2	3
Current in A (A)	45	65	85
Speed in mm/min (B)	200	400	600
Gas pressure in MPa (C)	0.6	0.7	0.8
Standoff distance in mm (D)	3	5	7

a surface profile's height characteristics. The Ra roughness's of the specimens were measured by Zeta 20 3D optical profiler in this study. Figure 7 shows the surface roughness (Ra) measurement results of experiment 13.

The energy and momentum of the plasma torch's high-velocity plasma jet melts, vaporizes, and removes the metal from the nozzle's impingement region. The plasma arc cutting nozzle was also analyzed via Zeta 20 3D optical profiler in this study. The nozzle of plasma arc cutting machine was placed on magnification objective in the vertical position for measuring by rotating the turret, for this case 5× objective was used, and Figure 8 shows the measurement of nozzle diameter results for experiment 7.

2.2.3 Optimization by hybrid ANN and GA

There are many possible types of ANN network architecture, but in this study back propagation (BP) learning was utilized. The BP network is the most extensively used because it has the advantage of learning and storing the mapping between any number of input and output layers without requiring sophisticated mathematical equations to define the mapping connection. Based on the training and back propagation of samples, BP can iteratively compute the network's weight coefficients and thresholds, lowering the network's error sum of squares [26]. The neural network was trained to perform a certain function by changing the values of the weights (connections) between elements. Typically, neural networks were modified or trained so that a certain input result in a certain output. Connection modes, weights, and activation functions all influence the ANN model's output, which can be stated as in equation (1) [27]:

$$y = f\left(\sum_j w_{ij}x_j + b\right) \tag{1}$$

where, f represents activation function, w represents weight value, x represents input vector, and b represents bias value.

In this study, two popular metrics were utilized to assess the forecasting performance the ANN model. The first was mean-squared error (MSE); it represents the average squared difference between the experimental values and the network outputs, which is a simple way of calculating the average difference in data. A low value of MSE often indicates a high-accuracy forecast. The MSE

Table 3. Mass and time results.

	Parameters/levels				Measurement			
Exp.	A	B	C	D	MB[1](kg)	MA[2](kg)	ML[3](kg)	Time (s)
1	45	200	0.6	3	2.67	2.508	0.162	54.05
2	45	200	0.6	3	2.508	2.33	0.178	54.2
3	45	200	0.6	3	2.33	2.205	0.125	53.78
4	45	400	0.7	5	2.66	2.526	0.134	26.7
5	45	400	0.7	5	2.526	2.354	0.172	27.1
6	45	400	0.7	5	2.354	2.225	0.129	26.74
7	45	600	0.8	7	2.645	2.535	0.11	17.54
8	45	600	0.8	7	2.535	2.395	0.14	17.81
9	45	600	0.8	7	2.395	2.235	0.16	18.07
10	65	200	0.7	7	2.62	2.47	0.15	54.23
11	65	200	0.7	7	2.47	2.307	0.163	54.12
12	65	200	0.7	7	2.307	2.160	0.147	53.81
13	65	400	0.8	3	2.675	2.521	0.154	27.25
14	65	400	0.8	3	2.521	2.38	0.141	27.1
15	65	400	0.8	3	2.38	2.245	0.135	26.8
16	65	600	0.6	5	2.65	2.51	0.14	17.8
17	65	600	0.6	5	2.51	2.35	0.16	18.22
18	65	600	0.6	5	2.35	2.215	0.135	17.69
19	85	200	0.8	5	2.655	2.527	0.128	53.92
20	85	200	0.8	5	2.527	2.375	0.152	54.28
21	85	200	0.8	5	2.375	2.225	0.15	54.21
22	85	400	0.6	7	2.68	2.543	0.137	26.54
23	85	400	0.6	7	2.543	2.372	0.171	27.08
24	85	400	0.6	7	2.372	2.220	0.152	26.72
25	85	600	0.7	3	2.7	2.55	0.15	17.87
26	85	600	0.7	3	2.55	2.389	0.161	17.95
27	85	600	0.7	3	2.389	2.260	0.129	17.53

[1]MB = Mass before cutting.
[2]MA = Mass after cutting.
[3]ML =Mass loss during cutting.

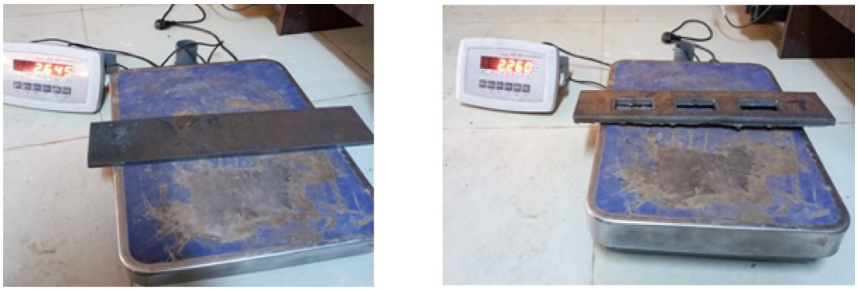

(a) before cutting (b) after cutting

Fig. 6. Mass measurement.

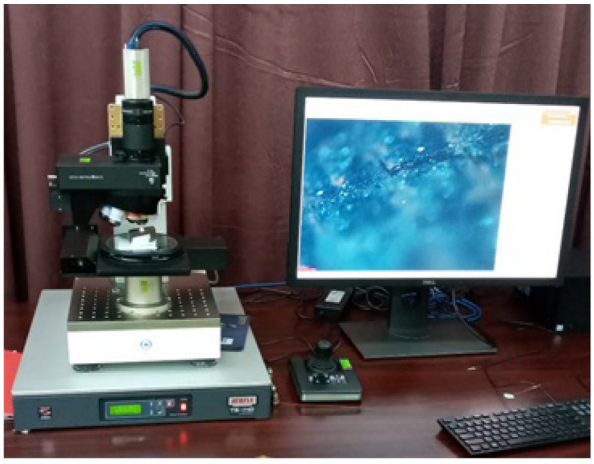

(a) measuring surface roughness

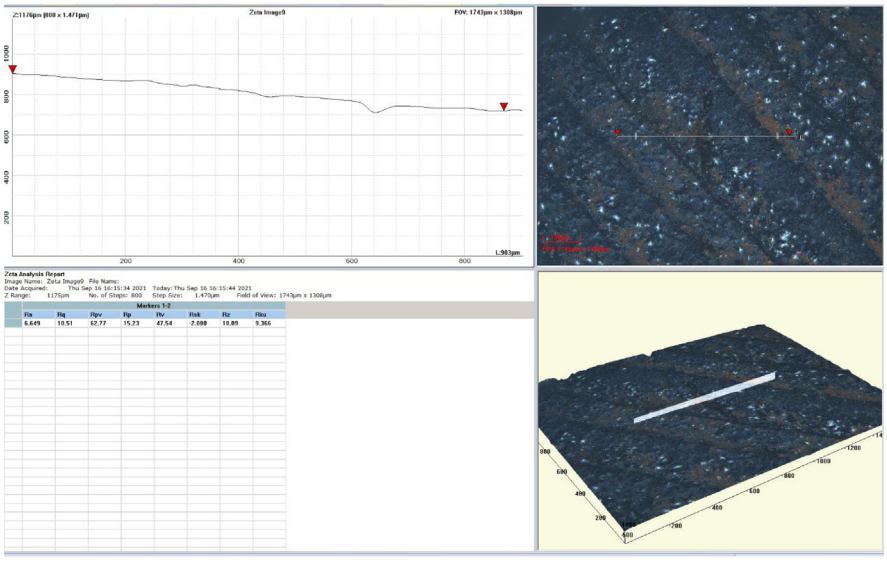

(b) surface roughness result of Exp. 13

Fig. 7. Zeta 20 3D optical profiler while measuring surface roughness.

can be written as follows in equation (2) [27].

$$MSE = \frac{1}{q}\sum_{k=1}^{q}[y(k) - t(k)]^2 \tag{2}$$

where, $t(k)$ and $y(k)$ and represent the experiment data and prediction value, respectively, and q is number of data.

The regression was another performance indicator for network efficiency shown in equation (3) [27]. The association between outputs and goals was measured using regression coefficients. It is a correlation coefficient (R) between the forecasts is the other metric. A deterministic relationship is represented by an R-value of 1; a random relationship is represented by an R-value of 0. A greater R-value was expected for an ANN model.

$$R = \frac{(y-\overline{y})(t-\overline{t})^T}{\sqrt{(y-\overline{y})(y-\overline{y})^T}\sqrt{(t-\overline{t})(t-\overline{t})^T}} \tag{3}$$

where, $\bar{t}$ and $\bar{y}$ are the mean values of the experiment data and prediction, respectively.

For getting good ANN model, the weights of the model should be optimized [28]. This includes obtaining of low MSE error. In this study, the developed ANN model was optimized by GA. By defining the interval of decision variables and the objective function, as well as applying the termination criteria and constraints in an iterative loop, the population of number of responses by the respective operators was constantly updated, and consequent generations with more satisfactory fitness values were obtained. The procedures of cutting parameters' optimization using ANN and GA is represented using the flowchart as shown on Figure 9.

3 Results and discussions

The experiment was conducted as per L27, and 27 specimens from 10 mm thickness of AISI 1020 mild steel

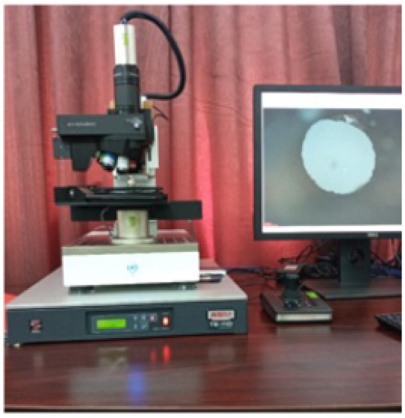

(a) measuring nozzle diameter

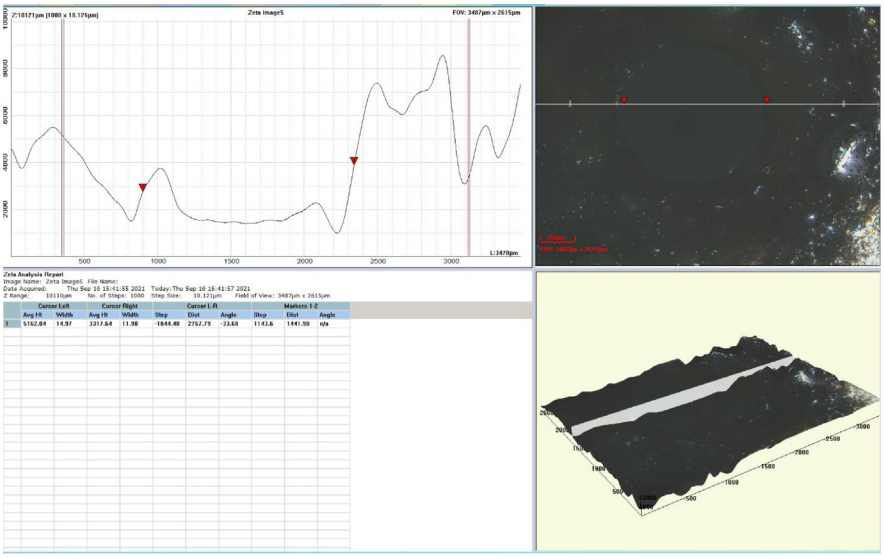

(b) nozzle diameter of Exp. 7

Fig. 8. Zeta 20 3D optical profiler while measuring nozzle diameter.

plate were cut. The final cut specimens that were obtained by varying cutting process parameters of the CNC EDON 100 plasma cutting machine are shown on Figure 3b. And then, the MRR was calculated using the measured mass before and after cutting specimen in a taken time listed on Table 3 and surface roughness (SR) were measured from these specimens. Nozzle orifice diameter was also measured after cutting each specimen. All the measured values of responses for surface roughness, material removal rate and nozzle diameter are shown on Table 4, and these results were also plotted as shown on Figure 10 to easily understand each experimental result relatively. As it is observed fro this figure, responses did not have common good outcomes for different parameters' setting of levels. Besides, the highest obtained values of MRR, SR and nozzle orifice diameter that were obtained from the trial experiments were 8.96 g/s, 15.734 µm and 1.4637 mm, respectively; whereas, the lowest obtained values of MRR, SR and nozzle orifice diameter were 2.324 g/s, 5.98 µm and 1.2114 mm, respectively.

3.1 Effects of cutting parameters on responses

3.1.1 Effects of current

As current increased, material removal rate increased whereas nozzle orifice diameter decreased. So, the increment of current showed that good outcomes for the two responses. However, surface roughness did not show linear relationship with current since when current increased surface roughness decreased and then increased. The cause for increment of roughness after 65 A of current might be more heat and plasma induced. These effects of current for the three responses are shown on Figure 11.

3.1.2 Effects of cutting speed

As shown on Figure 12, material removal rate increased whereas surface roughness decreased when cutting speed increased. So, the increment of cutting speed showed that good outcomes for the two responses and these are expected results. However, nozzle orifice diameter did not show

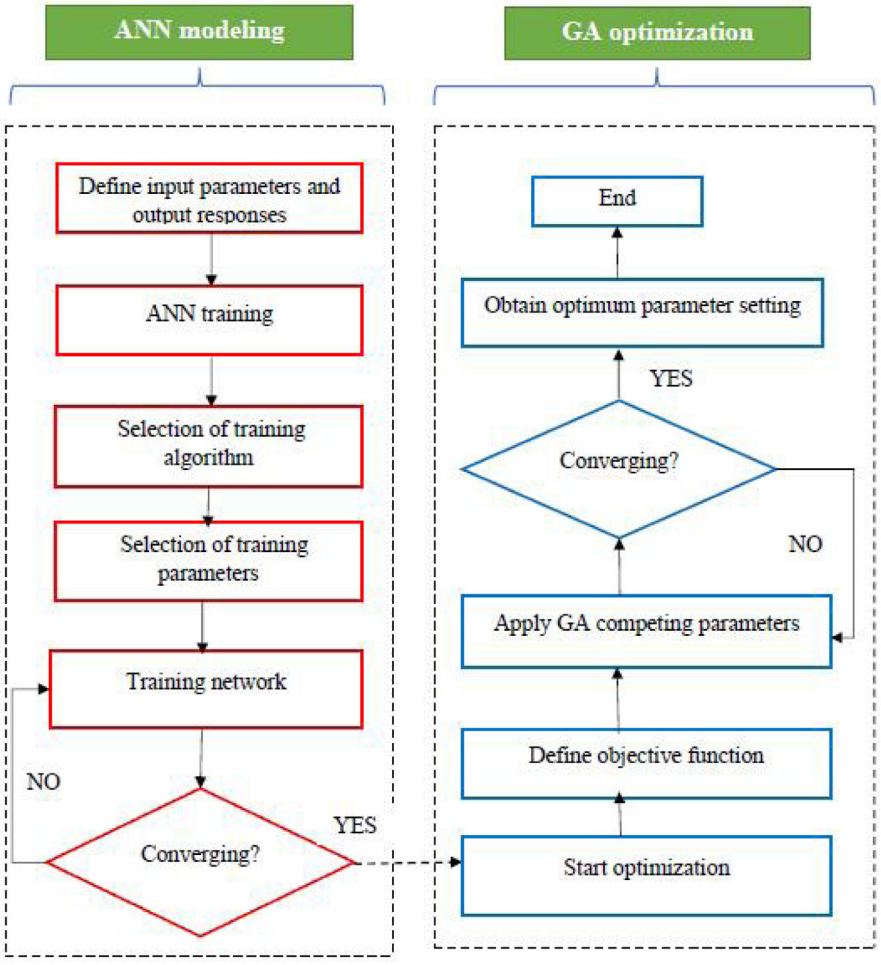

Fig. 9. Flowchart of hybrid ANN and GA optimization method [23].

linear relationship with cutting speed since as cutting speed increased, nozzle orifice diameter increased until speed reached at 400 mm/min and then decreased. The nozzle orifice diameter decreased at higher cutting speed might be due to the heat loss as cutting torch moves fast and the melted metal might close the orifice.

3.1.3 Effects of standoff distance

As shown on Figure 13, when standoff distance increased the following effects occurred. 1. Material removal rate decreased and then increased, 2. Surface roughness increased and then decreased, and 3. Nozzle orifice diameter change decreased slightly and then increased. Both material removal rate and nozzle diameter showed lower values at closed gap between torch and work-piece due to the possible occurrence of short circuit in flow of current across the gap.

3.1.4 Effects of gas pressure

As shown on Figure 14, all material removal rate, surface roughness and nozzle orifice diameter change decreased when gas pressure increased. So, the increment of gas pressure showed that good outcomes for surface roughness and nozzle orifice diameter. As pas pressure increases, there might occur drift on the concentrated or focused heat on the workpiece area where to be cut; as a result, there would not be obtained enough heat to melt the workpiece and nozzle tip.

It was observed that as shown on Figures 11, 12, 13, and 14, all three responses did not have the same effects as values of the cutting parameters' levels increased, and the setting of levels of the cutting parameters were not found the same as the highest experimental results shown on Table 4 and Figure 10. based on these, optimization of the cutting parameters of the plasma arc cutting process of AISI 1012 mild steel plate using multi-objective method was done to find the possible optimal levels of parameters. Therefore, the hybrid ANN and GA method was applied to optimize the cutting parameters and its implementation phases are summarized in Figure 9.

3.2 Optimization of cutting parameters

3.2.1 ANN modeling

In ANN modeling, determining the input or output data using process simulation, dividing it into training, evaluating, and confirming the ANN model, and normalizing it within the defined range were needed. And, creating

Table 4. All values of responses.

	Parameters/levels				Responses		
Exp.	A	B	C	D	MRR[1] (g/s)	SR[2] (Ra) (μm)	ND[3] (mm)
1	45	200	0.6	3	2.997	15.734	1.3965
2	45	200	0.6	3	3.284	14.96	1.3965
3	45	200	0.6	3	2.324	14.242	1.3965
4	45	400	0.7	5	5.019	13.37	1.4473
5	45	400	0.7	5	6.347	12.864	1.4473
6	45	400	0.7	5	4.824	12.117	1.4473
7	45	600	0.8	7	6.271	9.578	1.4419
8	45	600	0.8	7	7.860	8.340	1.4419
9	45	600	0.8	7	8.854	8.154	1.4419
10	65	200	0.7	7	2.766	6.971	1.4257
11	65	200	0.7	7	3.011	7.215	1.4257
12	65	200	0.7	7	2.731	7.43	1.4257
13	65	400	0.8	3	5.651	6.649	1.3802
14	65	400	0.8	3	5.202	6.132	1.3802
15	65	400	0.8	3	5.03	5.98	1.3802
16	65	600	0.6	5	7.865	8.631	1.3838
17	65	600	0.6	5	8.781	7.73	1.3838
18	65	600	0.6	5	7.63	8.55	1.3838
19	85	200	0.8	5	2.374	12.35	1.2114
20	85	200	0.8	5	2.8	12.89	1.2114
21	85	200	0.8	5	2.803	11.753	1.2114
22	85	400	0.6	7	5.162	11.33	1.4637
23	85	400	0.6	7	6.315	11.634	1.4637
24	85	400	0.6	7	5.688	10.455	1.4637
25	85	600	0.7	3	8.39	8.97	1.2834
26	85	600	0.7	3	8.96	8.386	1.2834
27	85	600	0.7	3	7.35	7.74	1.2834

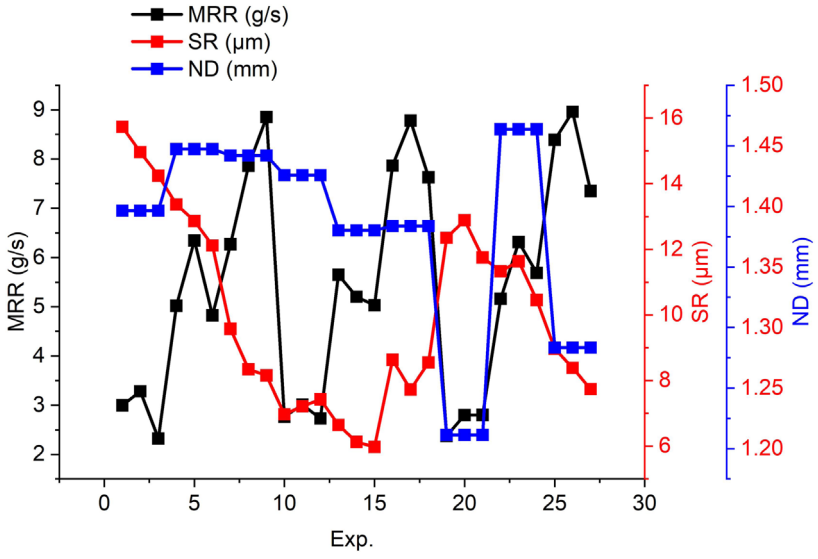

Fig. 10. Experimental results of responses.

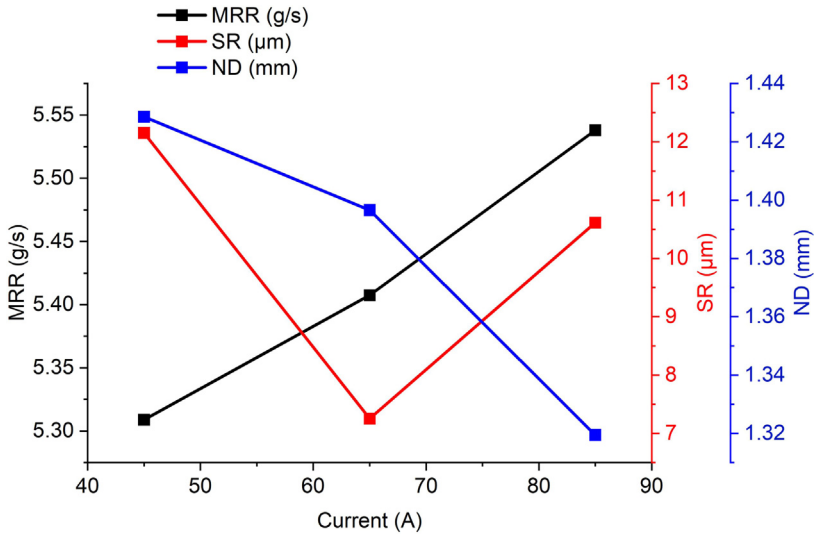

Fig. 11. Effects of current.

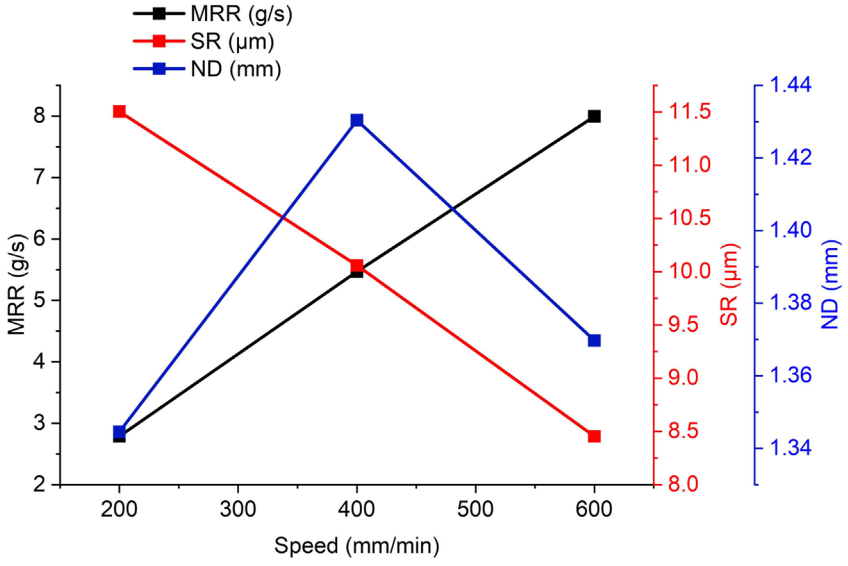

Fig. 12. Effects of cutting speed.

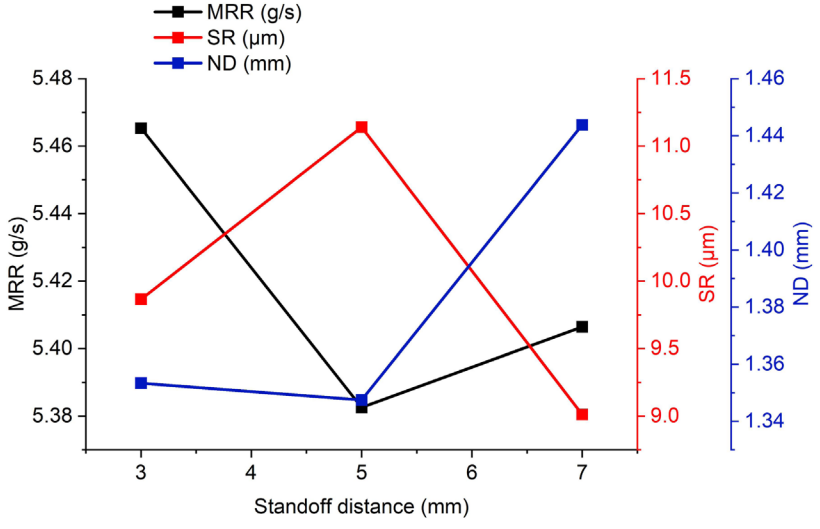

Fig. 13. Effects of standoff distance.

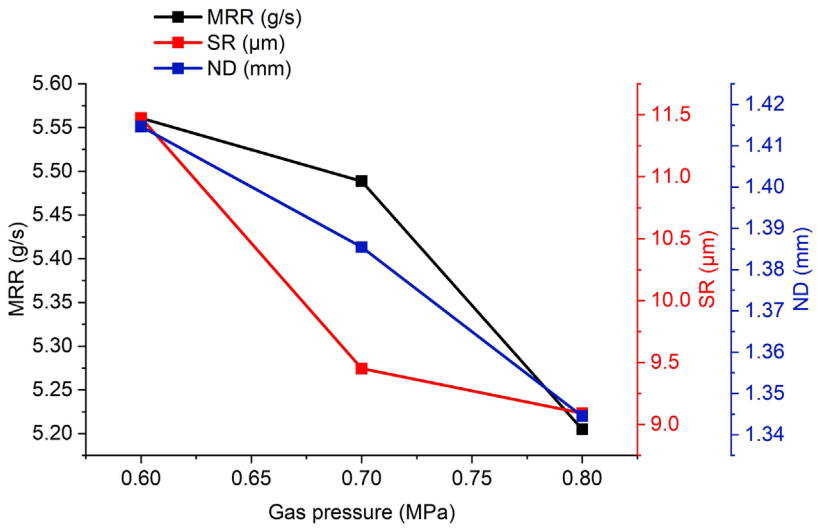

Fig. 14. Effects of gas pressure.

Table 5. Tested networks for getting the best model.

Name of ANN model	Network model	Learning algorithm	MSE	R
ANN-1	4-5-3	Levenberg-Marquardt	1.6768e-1	0.9904
ANN-2	4-6-3	Levenberg-Marquardt	1.34247e-1	0.9932
ANN-3	4-7-3	Levenberg-Marquardt	1.13607e-1	0.9911
ANN-4	4-8-3	Levenberg-Marquardt	2.00069e-1	0.9842
ANN-5	4-9-3	Levenberg-Marquardt	1.06885e-1	0.9932

the neural network design, including the output, hidden and input layers, as well as the total hidden layer neurons, hidden layers, activity functions, and training procedures were also carried out [29]. In this study, the learning strategy was based on the neural network of back propagation (BP) with Levenberg Marquardt algorithm among the available train functions of BP to get the best prediction results. The Levenberg-Marquardt algorithm is a method designed for sum-of-squared-error functions. The training time is exceedingly fast when training neural networks using this method on such errors.

The performances of the ANN model which were MSE and R were computed as shown in Table 5, and the influences of neurons number on the performance of the ANN model are shown. And, the result showed that a model having nine number of neurons has been selected since it has low MSE and high R-value almost near to one value. Having nine numbers of neurons had a required combination value of MSE and R relative to the other network models. The specification of the selected network model is shown on Table 6. ANN model having four input layer, one hidden layer with nine number of neurons and three output layers were selected as the best among the computed ANN models and the developed structure is shown on Figure 15.

3.2.2 GA based optimization

Several researchers have combined predictive models with optimization algorithms to improve industrial processes [30]. Determining the optimization process' constant parameters, such as population size, the number of decision variables, crossover fraction, and mutation rate were the next process. This value was set to default value on MATLAB 2020 software. The trained ANN determined each response's output value, and the objective function determined the fitness of the responses. In this stage, weight optimization was occurred, new weights were extracted by changing the constant parameters and MSE error for weight were calculated. Finally, using the selection function, the parents were chosen for the following stage after sorting the responses [23,31–33]. The fitness of all initial populations was calculated using the fitness function based on the neural network model, which was produced at random. Then, to generate a new generation, selection, crossover, and mutation were used as shown on Table 7. There are various advantages for choosing a tournament selection function, among them tournament selection is unaffected by the genetic algorithm fitness function's scaling, it is simple to code, works on parallel architectures, and allows for easy adjustment of the

Table 6. Specification of 4-9-3.

No.	Parameters	Value
1	Network configuration	4-9-3
2	Number of hidden layers	1
3	Number of hidden neurons	9
4	Transfer function used	Tansig
5	Amount of data utilized for training (%)	70
6	Amount of data utilized for testing (%)	15
7	Amount of data utilized for validation (%)	15
8	Learning rule	Levenberg-Marquardt
9	MSE	1.06885e-1
10	R	0.99318

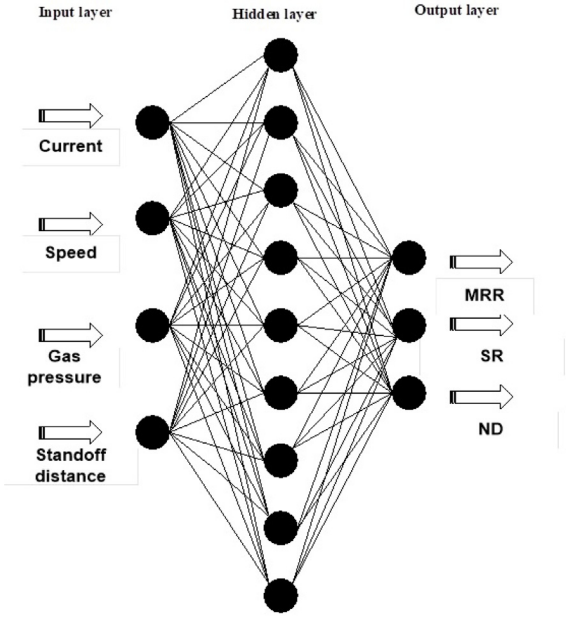

Fig. 15. Selected 4-9-3 ANN model.

Table 7. Objective function alternatives for GA.

Trial	Population size	Selection function	Cross over fraction	Mutation rate
1	50	Tournament	0.8	0.01
2	100	Tournament	0.5	0.02

selection pressure. Trial 2 with population size 100, cross over fraction 0.5 and 0.02 of mutation rate was selected among the two trials, due to having better fitness. After optimization was completed, the optimal point was determined by the highest response to the response ranking. As a result, the best optimal results of the cutting parameters of plasma arc cutting process while cutting AISI 1012 mild steel to improve MRR, SR and ND are shown on Table 8.

3.3 Confirmation tests

After the optimization procedure was completed, a confirmation test was performed to ensure that the analysis was accurate. This confirmatory test included utilization of the approximated values of optimal process parameters as input for cutting three $60 \times 30 \times 10$ mm AISI 1012 mild steel from $400 \times 90 \times 10$ plate. Three confirmatory tests were done, and the results are shown on Table 9. The results of the confirmation test were computed with

Table 8. Optimal process parameters obtained from GA.

No.	A (A)	B (mm/min)	C (MPa)	D (mm)	MRR (g/s)	SR (μm)	ND (mm)
1	73.9764	444.325	0.7998	3.1185	7.0032	4.2062	1.3142

Table 9. Confirmation result.

No.	A (A)	B (mm/min)	C (MPa)	D (mm)	MRR (g/sec)	SR (μm)	ND (mm)
1	74	444	0.8	3	7.0394	4.1208	1.4249
2	74	444	0.8	3	6.7592	4.3356	1.3586
3	74	444	0.8	3	6.9756	4.5724	1.3273
Average					6.9247	4.3429	1.3703
Error (%)					1.121	3.250	4.269

different studies [34–37] for verifying the results. This comparison helped to certain the obtained values were on the range of acceptable results. Actually, the accuracy of the errors depends on the tools and machines that were used to conduct the experiment and measure the responses. In this study, the optimal values of levels of the cutting parameters that were obtained using GA values listed on Table 8 of standoff distance, gas pressure, speed and current were taken with feasible values as 3 mm, 0.8 MPa, 444 mm/min and 74 A, respectively when the confirmation experiments were conducted. And then, the errors between the confirmatory experimental results and predicted responses' values were obtained 4.269%, 1.121% and 3.25% for ND, MRR and SR, respectively as shown on Table 9. All errors were found within the range of acceptable minimal values. Therefore, the obtained optimal levels of cutting parameters were acceptable to increase material removal rate and to reduce surface roughness and nozzle orifice diameter change.

4 Conclusion

In cutting of AISI 1020 mild steel plate using CNC plasma arc cutting machine was difficult, due to the combined effect of a continuous failure of the nozzle and getting low quality of the edge of cut plate. To address these issues, this study aimed to optimize CNC plasma arc cutting factors such as standoff distance, current, gas pressure, and cutting speed using a hybrid ANN-GA method to improve removal rate of material, surface roughness, and nozzle orifice diameter change while cutting AISI 1020 mild steel mild steel plate, and the following conclusions were drawn.

- The cutting parameters of the CNC plasma arc cutting process on cutting AISI 1020 mild steel grade plate by demonstrating the effects of various input parameters' levels on the material removal rate, Ra surface roughness and nozzle orifice diameter were optimized. For the experiment, three levels of variation were taken to the four input parameters of current, cutting speed, standoff distance, and gas pressure. Twenty-seven experiments were carried out using Taguchi's L27 orthogonal array approach. In this experimental investigation, the highest material removal rate (MRR) of 8.96 g/s, Ra surface roughness (SR) of 15.734 μm and nozzle orifice diameter (ND) of 1.4637 mm were achieved, whereas the lowest obtained values of MRR, SR and ND were 2.324 g/s, 5.98 μm and 1.2114 mm, respectively.
- In these experimental results, the highest MRR of 8.96 g/s was achieved at 85 A of current, 600 mm/min of cutting speed, 0.7 MPa of gas pressure and 3 mm of standoff distance. The lowest SR value of 5.98 μm was obtained at 65 A of current, 400 mm/min of cutting speed, 0.8 MPa of gas pressure and 3 mm of standoff distance. Besides, the ND value of 1.2114 mm was obtained after cutting the plate at 85 A of current, 200 mm/min of cutting speed, 0.8 MPa of gas pressure and 5 mm of standoff distance.
- As the three responses were observed from the trial experiments, they did not have a common parameters' setting of levels to achieve the desired outcomes. As a result, optimization of the plasma arc cutting process while cutting AISI 1020 mild steel plate was done.
- The MRR, SR and ND results of plasma arc cutting of AISI 1020 mild steel plate were predicted and optimized using an ANN-GA hybrid model created in this study. The results indicated that the ANN model could predict the outputs with MSE of 1.06885e–1. During the ANN training of the model, a 4-9-3 network trained with Levenberg-Marquardt algorithm was used to have the greatest prediction capability and was considered for subsequent GA optimization.
- The developed ANN model was successfully linked with GA for optimizing the cutting parameters. During iterations of GA optimization, when the stall generation condition was met, the quest came to an end. The GA optimization output provided the optimum MRR of 7.0032 g/s, SR of 4.2062 μm and ND of 1.3142 mm with corresponding values of cutting parameters of current of

73.9764 A, cutting speed of 444.325 mm/min, gas pressure of 0.7998 MPa and standoff distance of 3.1185 mm.
– Finally, confirmatory experiments were conducted using the feasible optimal levels of cutting parameters (74 A of current, 444 mm/min of cutting speed, 0.8 MPa of gas pressure and 3 mm of standoff distance) to verify the optimal parameters. From the confirmation experiment, the average results of 6.9247 g/s of MRR, 4.3429 μm of SR and 1.3703 mm of ND were obtained. There were minimal percentage of errors between the ANN-GA predicted optimal responses' results and the confirmatory experimental results that were found 1.121%, 3.250% and 4.269% for MRR, SR and ND, respectively.
– Wear rate, type of wear and life of nozzle were not investigated and analyzed using SEM and experimentally, so these issues might be the future outlooks for researchers.

Nomenclature

$\bar{t}$	Mean values of the experiment data
$\bar{y}$	Mean values of the prediction
b	Bias value
f	Activation function
q	Number of data
t	Experiment data
w	Weight value
x	Input vector
y	Prediction value
AISI	American iron and steel institute standard
AMIMTDE	Amhara metal industry and machine technology development enterprise
ANN	Artificial neural network
ANOM	Analysis of mean
ANOVA	Analysis of Variance
BP	Back propagation
CAD	Computer aided design
CNC	Computer numerical control
DOE	Design of experiment
EN	European standard steel number
GA	Genetic algorithm
HAZ	Heat affected zone
L16	Orthogonal array of Taguchi design with 16 runs
L27	Orthogonal array of Taguchi design with 27 runs
L9	Orthogonal array of Taguchi design with 9 runs
MA	Mass after cutting
MB	Mass before cutting
ML	Mass loss during cutting
MRR	Material removal rate
MSE	Mean squared error
ND	Nozzle orifice diameter
R	Correlation coefficient
Ra	Roughness average
RSM	Response surface methodology
S/N	Signal-to-noise
SR	Surface roughness

Funding

There was not any fund for this research.

Author contributions

All authors contributed equally to this work.

Conflicts of interest/Competing interests

No conflicts of interest for this research.

Availability of data and material

All necessary data are found in the research paper.

References

1. M. Siva Kumar, D. Rajamani, E. Abouel Nasr, E. Balasubramanian, H. Mohamed, A. Astarita, A hybrid approach of anfisartificial bee colony algorithm for intelligent modeling and optimization of plasma arc cutting on monelâ 400 alloy, Materials **14**, 6373 (2021)
2. K. Salonitisa, S. Vatousianos, in *45th CIRP Conference on Manufacturing Systems 2012* (Elsevier, 2012), pp. 287–292
3. P. Patel, S. Soni, N. Kotkunde, N. Khanna, Study the effect of process parameters in plasma arc cutting on quard-400 material using analysis of variance, Mater. Today: Proc. **5**, 6023–6029 (2018)
4. M. Gostimirović, D. Rodić, M. Sekulić, A. Aleksić, An experimental analysis of cutting quality in plasma arc machining, Adv. Technol. Mater. **45**, 1–8 (2020)
5. D. Rajamani, K. Ananthakumar, E. Balasubramanian, J. Paulo Davim, Experimental investigation and optimization of pac parameters on monel 400 superalloy, Mater. Manuf. Process. **33**, 1864–1873 (2018)
6. M.R.C. Bidajwala, M.M.A. Trivedi, M.H.M. Gajera, M.T.S. Raol, Parametric optimization on plasma arc cutting machine for aisi 1018, Scientific Journal of Impact Factor (SJIF) 3 (2015)
7. S.R. Mangaraj, D.K. Bagal, N. Parhi, S.N. Panda, A. Barua, S. Jeet, Experimental study of a portable plasma arc cutting system using hybrid rsm-nature inspired optimization technique, Mater. Today: Proc. **50**, 867–878 (2022)
8. S. Mittal, M. Mahajan, Multi-response parameter optimization of cnc plasma arc machining using Taguchi methodology, J. Ind. Eng.**11**, (2018)
9. K.R.P. Pallavi H. Agarwal, Optimizing plasma arc cutting parameters for structural steel using grey relational analysis, Int. J. Eng. Res. Technol. **8**, (2019)
10. S. Sharma, M.K. Gupta, R. Kumar, N. Bindra, Experimental analysis and optimization of process parameters in plasma arc cutting machine of en-45a material using Taguchi and Anova method, Int. J. Mech. Aerospace Ind. Mechatron. Manuf. Eng. **11**, 1387–1391 (2017)
11. D.B. Ghane, Optimization of design parameters and nozzle wear on cnc plasma machine by experimentation, Int. Res. J. Eng. Technol. (IRJET) **6**, (2019)

12. E. Agbonoga, O. Adedipe, U. Okoro, F. Usman, O. Kafayat, S. Lawal, Effect of process parameters on the surface roughness and kerf width of mild steel during plasma arc cutting using response surface methodology, FUOYE J. Eng. Technol. **5**, (2020). https://doi.org/10.46792/fuoyejet.v5i1.464
13. G. Singh, S. Akhai, Experimental study and optimization of mrr in cnc plasma arc cutting, J. Eng. Res. Appl. **5**, (2015)
14. P. Pittayachaval, Y. Aupkaew, S. Sakhonkhan, T. Sukan, C. Patchaikhonang, Investigating plasma-nozzle wear based on processing time and current ampere, Mater. Sci. Forum **987**, 171–176 (2020)
15. H. Pothur, V. Reddy, R. Ganesan, Experimental investigations on process parameters of stainless steel 410 alloy by plasma arc machining process using grey relational analysis with entropy measurement, Mater. Today: Proc. **62**, 559–565 (2022)
16. A. Belhocine, D. Shinde, R. Patil, Thermomechanical coupled analysis-based design of ventilated brake disc using genetic algorithm and particle swarm optimization, JMST Adv. (2021). https://doi.org/10.1007/s42791-021-00040-0
17. H. Patel, H. Gohil, N. Vasawala, J. Patel, Experiment and analyse material removal rate in plasma arc cutting of ss410 for various parameters using Anova, Int. J. Adv. Eng. Manag. 5(2), 179–187 (2023)
18. T.K. Gupta, K. Raza, Optimization of ann architecture: a review on nature-inspired techniques, Mach. Learn. Bio-Signal Anal. Diag. Imaging (2019)
19. A. Equbal, M. Shamim, I.A. Badruddin, M.I. Equbal, A.K. Sood, N.N. Nik Ghazali, Z.A. Khan, Application of the combined ann and ga for multi-response optimization of cutting parameters for the turning of glass fiber-reinforced polymer composites, Mathematics **8**, (2020)
20. J. Carr, An introduction to genetic algorithms (2014). https://scholar.google.com/scholar?hl=en&as_sdt=0%2C5&as_ylo=2016&as_yhi=2016&q=Carr%2C+J.%2C+An+Introduction+to+Genetic+Algorithms.+2014&btnG=
21. J. Roberts, A. Cassula, J. Silveira, P. Prado, J. Freire, Gatoolbox: a matlab-based genetic algorithm toolbox for function optimization, in: The 12th Latin-American Congress on Electricity Generation and Transmission – Clagtee, 2017
22. M.A. Linger, T.M. Bogale, Parameters optimization of tungsten inert gas welding process on 304l stainless steel using grey based Taguchi method, Eng. Res. Express **5**, (2023)
23. A.K. Mengistie, T.M. Bogale, Development of automatic orbital pipe mig welding system and process parameters'^{TM} optimization of aisi 1020 mild steel pipe using hybrid artificial neural network and genetic algorithm, Int. J. Adv. Manuf. Technol. (2023). https://doi.org/10.1007/s00170-023-11796-1
24. E.A. Berihun, T.M. Bogale, Parameter optimization of pet plastic preform bottles in injection molding process using grey-based Taguchi method, Adv. Mater. Sci. Eng. 2022, (2022)
25. H. Ramakrishnan, R. Balasundaram, N.V. Ganesh, N. Karthikeyan, Experimental investigation of cut quality characteristics on ss321 using plasma arc cutting, J. Braz. Soc. Mech. Sci. Eng. **40**, 1–11 (2018)
26. C. Mu, B.Z. Qiu, X.H. Liu, A new method for figuring the number of hidden layer nodes in bp algorithm, Int. J. Recent Innov. Trends Comput. Commun. **5**, 101–114 (2017)
27. F. Yang, H. Cho, H. Zhang, J. Zhang, Y. Wu, Artificial neural network (ann) based prediction and optimization of an organic rankine cycle (orc) for diesel engine waste heat recovery, Energy Convers. Manag. **164**, 15–26 (2018)
28. S.H. Gökler, S. Boran, Determining optimal machine part replacement time using a hybrid ann-ga model, Sci. Iranica **29**, 771–782 (2022)
29. K.G. Sheela, S.N. Deepa, Review on methods to fix number of hidden neurons in neural networks, Math. Probl. Eng. **2013**, 11 (2013)
30. S. Masoudi, M. Mirabdolahi, M. Dayyani, F. Jafarian, A. Vafadar, M.R. Dorali, Development of an intelligent model to optimize heat-affected zone, kerf, and roughness in 309 stainless steel plasma cutting by using experimental results, Mater. Manuf. Process. **34**, 345–356 (2019)
31. A.E. Abere, A.A. Tsegaw, R.B. Nallamothu, Process parameters optimization of bobbin tool friction stir welding on aluminum alloy 6061-t6 using combined artificial neural network and genetic algorithm, J. Braz. Soc. Mech. Sci. Eng. **44**, 566 (2022)
32. E.W. Fenta, A.A. Tsegaw, in Artificial Intelligence and Digitalization for Sustainable Development: 10th EAI International Conference, ICAST 2022, Bahir Dar, Ethiopia, November 4–6, 2022, Proceedings (Springer, 2023), pp. 13–26
33. V. Khezri, E. Yasari, M. Panahi, A. Khosravi, Hybrid artificial neural networkâ genetic algorithm-based technique to optimize a steady-state gas-to-liquids plant, Ind. Eng. Chem. Res. **59**, 8674–8687 (2020)
34. S. Ahmad R.M. Singari, R.S. Mishra, Tri-objective constrained optimization of pulsating dc sourced magnetic abrasive finishing process parameters using artificial neural network and genetic algorithm, Mater. Manuf. Process. **36**, 843–857 (2021)
35. U.M.R. Paturi, S. Cheruku, V.P.K. Pasunuri, S. Salike, N. Reddy, S. Cheruku, Machine learning and statistical approach in modeling and optimization of surface roughness in wire electrical discharge machining, Mach. Learn. Appl. **6**, 100,099 (2021)
36. A.J. Santhosh, A.D. Tura, I.T. Jiregna, W.F. Gemechu, N. Ashok, M. Ponnusamy, Optimization of cnc turning parameters using face centered ccd approach in rsm and ann-genetic algorithm for aisi 4340 alloy steel, Results Eng. **11**, 100–251 (2021)
37. D. Yang, Q. Guo, Z. Wan, Z. Zhang, X. Huang, Surface roughness prediction and optimization in the orthogonal cutting of graphite/polymer composites based on artificial neural network, Processes **9**, 1858 (2021)

Citation de l'article : Nebyu Silabat Melaku, Teshome Mulatie Bogale, Parameters optimization in plasma arc cutting of AISI 1020 mild steel plate using hybrid genetic algorithm and artificial neural network, Int. J. Simul. Multidisci. Des. Optim. **14**, 20 (2023)